

Millimeter-Wave Spectra and Global Torsion–Rotation Analysis for the CH₃OD Isotopomer of Methanol

M. S. Walsh,* Li-Hong Xu,† R. M. Lees,* I. Mukhopadhyay,‡ G. Moruzzi,§ B. P. Winnewisser,¶ S. Albert,|| Rebecca A. H. Butler,|| and F. C. DeLucia||

*Department of Physics, University of New Brunswick, Fredericton, New Brunswick, Canada E3B 5A3; †Department of Physical Sciences, University of New Brunswick, Saint John, New Brunswick, Canada E2L 4L5; ‡Laser Programme, Centre for Advanced Technology, Indore 452 013, India; §Dipartimento di Fisica dell'Università di Pisa and INFN, Via Filippo Buonarroti 2, I-56127 Pisa, Italy;

¶Physikalisch Chemisches Institut, Justus Liebig Universität, Heinrich Buff Ring 58, D-35392 Giessen, Germany; and

||Department of Physics, The Ohio State University, 174 West 18th Avenue, Columbus, Ohio 43210

Received May 31, 2000; in revised form July 6, 2000

New millimeter-wave and microwave measurements for CH₃OD have been combined with previous literature data and with an extended body of Fourier transform far-infrared observations in a full global analysis of the first two torsional states ($v_t = 0$ and 1) of the ground vibrational state. The fitted CH₃OD data set contained 564 microwave and millimeter-wave lines and 4664 far-infrared lines, representing the most recent available information in the quantum number ranges $J \leq 20$ and $K \leq 15$. A 53-parameter converged global fit was achieved with an overall weighted standard deviation of 1.060, essentially to within the assigned measurement uncertainties of ± 100 kHz for almost all of the microwave and millimeter-wave lines and ± 6 MHz for the far-infrared lines. The new parameters for CH₃OD are compared to previous results obtained for the ¹²CH₃OH, ¹³CH₃OH, and CD₃OH isotopomers over the same quantum number ranges using the identical fitting program. Strong asymmetry-induced coupling between the accidentally near-degenerate $0E$ and $-1E$ $v_t = 0$ substates is successfully modeled by the fit. © 2000 Academic Press

Key Words: methanol; CH₃OD; torsion; millimeter-wave spectra; far-infrared spectrum; global fitting.

I. INTRODUCTION

This analysis of the ground state spectrum of the CH₃OD species of methanol is the fourth in a series of global fitting studies of the microwave (MW), millimeter-wave (MMW), and far-infrared (FIR) spectra of methanol and its isotopomers (1–4). The data sets have all been chosen to cover closely similar ranges of quantum number to permit consistent inter-comparison of the results. Each of the global fits reproduces the data to within experimental accuracy, using a computer program (5) based on the formalism of Herbst *et al.* (6). Here, we will give brief introductory remarks relating to CH₃OD and refer the reader to the previous literature (1–7) for details of the computer program, the Hamiltonian model used, and the background to the notation for the torsion–rotation quantum numbers and transition labeling.

There have been a number of studies of the MW and MMW spectra of CH₃OD (8–13), originally aimed at the structural determination of methanol via isotopic substitution, and later with astrophysical applications in view. CH₃OD was also included in Woods' far-infrared (FIR) study of four methanol isotopomers (14), whose ground state spectra were subsequently analyzed by Kwan and Dennison (15) in order to better define the torsional potential and Hamiltonian parameters. Recently, the high-resolution Fourier transform far-infrared (FT-FIR) spectrum has been investigated for the ground vibrational

state, and several fits to model Hamiltonians of differing orders have been reported (16–19) for a variety of subsets of the FTFIR data. Further ground state information is also available in the form of IR combination differences from the spectrum of the CO–stretching fundamental band (20) and from exploration by laser Stark spectroscopy of torsion–rotation transitions in the vicinity of the HCN laser lines (21).

The present paper reports new MMW measurements for CH₃OD in the ranges from 126–147 and 482–499 GHz, plus a number of further measurements in the MW region, which have yielded about 160 new line assignments. These have been combined with previous data in a global fit of a total of 5228 assigned MW, MMW, and FTFIR ground state transitions of CH₃OD involving levels of the first two torsional states ($v_t = 0$ and 1) up to a maximum rotational quantum number J of 20. The one-dimensional torsion–rotation model is implemented in a well-tested computer program (5) previously applied successfully for the ¹²CH₃OH (1, 2), ¹³CH₃OH (3), and CD₃OH (4) isotopomers of methanol and also for acetaldehyde, CH₃CHO (7).

As described previously (4), the principal goals in our program of global analyses of ground state spectra for methanol isotopomers are as follows.

(i) To achieve fits of all observed transitions to within experimental accuracy over quantum number ranges sufficient for rigorous testing of the model. So far, our CH₃OH,

¹³CH₃OH, and CD₃OH analyses have proven that the one-dimensional Hamiltonian model is very successful in describing $v_r = 0$ and 1 methanol energy levels below and immediately above the torsional barrier.

(ii) To obtain molecular parameters for different methanol isotopomers in as consistent a way as possible by using the same computer program to analyze data sets covering the same quantum number ranges. This should then permit meaningful intercomparison in order to explore the physical interpretation of the parameters.

II. NEW MMW AND MW SPECTRA

The majority of the new measurements in this work were obtained in two runs on the automated FASSST rapid-scan MMW spectrometer at Ohio State University (22). The first scan covered the region from 126.4 to 146.9 GHz, generating a peak list of 567 lines, and the second from 482.5 to 499.0 GHz with a peak list of 253 lines. We found that even with the short scanning times of the FASSST technique, rapid D ↔ H chemical exchange in the absorption cell was a problem, as a significant number of known CH₃OH lines from the recent microwave review (23) turned up in the peak lists of the CH₃OD spectra. In addition to the new MMW observations, a number of additional lines have been measured in the MW region at the University of New Brunswick (24), using a conventional Stark-modulated spectrometer with klystron sources.

We have been able to assign torsion-rotation quantum numbers to a substantial number of the new lines. These transitions with their frequencies are included in the complete tables of assigned CH₃OD MW and MMW lines which are discussed below in Section III.3. As well, we have deposited the FASSST MMW peak lists, giving the line frequencies and relative intensities and marking the suspected CH₃OH features, as supplementary data with the JMS archive accessible through the JMS home page at www.idealibrary.com.

III. GLOBAL FIT

1. The $v_r = 0$ and 1 Data Set

Our fitted data set for CH₃OD included a total of 5228 MW, MMW, and FIR lines covering quantum number ranges $v_r \leq 1$ and $J \leq 20$ for both *A* and *E* torsional symmetries and all available *K* states. The 564 MW and MMW frequencies were obtained from the NIST MW data center compilation (25), previous literature (8–13), private files (26), and the new measurements discussed above from Ohio State and UNB (24). The 4664 fitted FTFIR data were derived from analysis, with the aid of the Ritz program (27), of spectra recorded in the Giessen laboratory (16, 17). For the Fourier transform measurements, the long integration times again meant that chemical exchange between D and H was a significant problem, and

strong CH₃OH lines can be seen in published segments of the FIR spectra (16, 18).

The present FTFIR dataset is about twice as large as has previously been analyzed, with a more complete range of *K* values, particularly for torsionally excited *E* transitions. Earlier reported fits (17, 19) were to a transition subset with $J \leq 20$ and $K \leq 6$, but included only *K* states from -3 to -6 for *E* subbands involving $v_r = 1$ levels. This previous data set, which was stated to contain 2348 lines in the 20–350 cm⁻¹ region, was archived as supplementary information and made available through both the British Library Document Supply Centre (17) and the JMS archive (19). (We note in passing, however, that the list from the former contains only 2306 entries, while the latter has 2348 transitions but includes around 50 wavenumbers below 20 cm⁻¹ which are duplicates of MW and MMW lines already in the fit. Also, the *A*[±] labeling is somewhat erratic in the archived data when the *K*-doubling is unresolved, and transitions are listed which formally are forbidden by the selection rules. With the *A*[±] splittings unresolved, of course, the forbidden and allowed transition wavenumbers are identical so that only the statistics of the fit are affected, with a single measured line being included up to four times. Nevertheless, one needs to be careful in reading *A*[±] transition labels from the archived data.)

In our data set, all of the transition information was critically evaluated for reliability and internal consistency prior to fitting; this step had proven decisive in the earlier analyses in removing contamination from poorly measured or misassigned lines and thereby achieving convergence and stable fits. All 564 MW and MMW lines were assigned an uncertainty of ±100 kHz in the fit, except for a few unresolved *K*-doublet transitions which were given uncertainties of ±200 kHz. The 4664 FTFIR lines were assigned a uniform uncertainty of ±0.0002 cm⁻¹ (±6 MHz). Here, use of the line-fitting routine developed for the Ritz program (28) was important in resolving blended features and enhancing the accuracy of the wavenumbers. A further group of assigned MW and MMW lines were excluded from the fit because the ($\nu_{\text{obs}} - \nu_{\text{calc}}$) residuals were unreasonably high or because they were blended and had multiple assignments. A number of FTFIR lines were omitted as well for the latter reason. In view of the large size and broad quantum number range of the overall fitted dataset, we do not believe that the omission of these doubtful lines would substantially affect the values of the fitted parameters.

We also chose at this stage not to incorporate $v_r = 2$ *a*-type MMW lines, which had been included in one of the previous studies (19), in order to maintain consistency and comparability with the earlier global fits in our series (1–4). To treat $v_r = 2$ data properly in a true $v_r = 0$ –2 fit, one would look for $\Delta K = \pm 1$ *b*-type transitions more sensitive to the torsional potential and seek to include data covering a substantial range of *J* and *K* quantum numbers. Such $v_r = 2$ data have so far only been treated in a single- v_r -state fit (18). In the present work, as discussed below in Section II.3, we did calculate the

$\nu_i = 2$ *a*-type transition frequencies utilizing our $\nu_i = 0 + 1$ parameter set to explore how well these parameters would account for that $\nu_i = 2$ information.

2. Overall Fit Results and Parameters

In the global fit to the CH₃OD data, we achieved convergence with an overall unitless weighted standard deviation of 1.060 using 53 adjusted parameters. The MW and MMW lines were fitted with weighted rms errors of 1.149 for the 424 $\nu_i = 0$ transitions and 1.816 for the 140 $\nu_i = 1$ transitions. The FTFIR lines were fitted with a weighted rms error of 1.011. Table 1 presents the parameters from the fit arranged according to increasing order of torsion–rotation operator. The overall order is $n \equiv l + m$, where l is the order of the torsional factor, and m is the order of the rotational factor (6). For comparison, the results from the previous corresponding fits for CH₃OH, ¹³CH₃OH, and CD₃OH (2–4) are included in Table 1 as well.

In general, the four sets of molecular constants show good consistency, with comparable values for the larger parameters allowing for changes with mass, and no obvious discrepancies in the lower order terms. As found for CD₃OH (4), the “*a*-type” parameters with a P^2 factor in their matrix elements decrease significantly with deuteration, but now the “*b*-type” terms with P_a -dependence such as k_1 or k_2 also change substantially, indicating that centrifugal distortion with axial K -rotation tends to be dominated by the light OH rotor.

In Table 1, we did not attempt to compare our parameters with those of other workers, due to a problem with contemporary detailed analyses of methanol spectra that the specific Hamiltonians used in the various studies almost all differ in some important aspect, with significant effects on the parameters. One of the major differences arises through the definition of the molecular axes. The torsional angular momentum P_γ in the commonly used IAM internal axis method (9, 15) corresponds in our rho-axis system (7) to the operator $(P_\gamma + \rho P_a)$, which leads to major changes in the expectation values of terms of the type P_γ^n and sizeable deviations between superficially identical Hamiltonian parameters. Thus, one must exercise great care in comparing the parameters from the different models. Recent discussion (29) of the possible reasons for large discrepancies between the k_1 , k_2 , and k_3 values in ¹³CH₃OH global fits, for example, should be revised because the differences between the two axis systems and Hamiltonians were not taken into account. If one transforms appropriately between the two axis systems, the parameters turn out to be closely similar.

3. CH₃OD MW and MMW Transitions

To partially display the range and quality of the global fit, we list all $\nu_i = 0 \leftarrow 0$ and $1 \leftarrow 1$ MW and MMW transitions that were considered in this work in Tables 2 and 3 for *A* and *E* torsional symmetries, respectively. The data are arranged by $K' \leftarrow K''$ subband, together with the $(\nu_{\text{obs}} - \nu_{\text{calc}})$ residuals and

the original literature references. About 160 of the lines are the new CH₃OD measurements from the FASSST spectrometer at Ohio State University (22) or the Stark spectrometer at UNB. The literature lines marked with an asterisk in the tables were not included in the fit because they violated closed-loop combination relations, had unreasonably large (O – C) residuals, or were blended with multiple assignments.

For the quantum number ranges covered in this work, the accuracies of line predictions based on the final parameter set of Table 1 will be either ~ 100 kHz or ~ 6 MHz depending on whether frequency-measured or Fourier transform FIR data were fitted in the original data set. Thus, the ranges of the MW and MMW data in Tables 2 and 3 also serve as guides as to whether a given calculated transition may be expected to have the higher 100 kHz level of accuracy. The uncertainties in calculated frequencies increase sharply above the fit upper limit of $J = 20$.

To explore whether $\nu_i = 2$ *a*-type data were predictable from our $\nu_i = 0 + 1$ parameter set or whether they contained significant new information that would require further higher order parameters, we calculated frequencies for the known $\nu_i = 2$ MW lines. The results are presented in Table 4 and show that our parameters do a reasonably good job of accounting for the $\nu_i = 2$ data. However, the (O – C) errors are relatively systematic and increase fairly linearly with J' to typically about 6 MHz at $J' = 10$, suggesting that refinements or additions to the J -dependent terms in the Hamiltonian would indeed improve the agreement. The very large residuals obtained for the $K = -4$ *E* transitions indicate a possible misassignment of that series in the literature.

4. Coupling between the $K = 0$ and -1 *E* States

One of the notable features of the energy level structure of CH₃OD is an accidental near-degeneracy between the $K = 0$ and $K = -1$ *E* levels for $\nu_i = 0$, leading to particularly strong asymmetry-induced coupling and mixing among the low- K *E* levels. Due to partial cancellation of torsional and rotational energies, the $K = -1$ *E* levels lie only about 0.6 cm^{-1} above the $K = 0$ *E* levels at low J . Furthermore, the large CH₃OD value for the product of inertia term, D_{ab} , gives a large $\Delta K = 1$ asymmetry matrix element coupling the $K = 0$ and -1 levels. Thus, when the $\Delta K = 2$ asymmetry matrix elements connecting to the $K = 1$ and $K = \pm 2$ *E* levels not far above are brought in as well, strong mixing occurs throughout the whole 5×5 $K = 0 - \pm 2$ sublevel complex with significant perturbations to transition frequencies and intensities. With the resulting difficulties in assignment, the energies for these $\nu_i = 0$ *E* substates have been determined from the FTFIR spectrum so far only up to $J = 18$ for $K = 0$ and -1 , $J = 17$ for $K = 1$ and 2 , and $J = 14$ for $K = -2$. In Fig. 1a, we show the pattern of the experimental energies in J -reduced form, obtained by subtracting $BJ(J + 1)$ from the term values using a mean effective B value of 0.7576 cm^{-1} . The close approach

TABLE 1
Torsion-Rotation Parameters (in cm⁻¹) for Global Fits of Transitions Involving $v_t = 0$ and $v_t = 1$ Torsional States of CH₃OH, ¹³CH₃OH, CD₃OH, and CH₃OD

Term Order nlm ^a	Operator ^b	Parameter ^b	Methanol Global Fit Parameters ^c			
			CH ₃ OH (Ref. 2)	¹³ CH ₃ OH (Ref. 3)	CD ₃ OH (Ref. 4)	CH ₃ OD (Present Work)
220	(1-cos3γ)/2	V ₃	373.594(7)	373.77677(10)	370.0549(2)	366.3400(1)
	P _γ ²	F	27.64682(2)	27.641920(9)	24.993957(5)	17.42806(1)
211	P _γ ³ P _a	ρ	0.81020601(1) ^d	0.81016448(4) ^d	0.89466007(7) ^d	0.6993443(2) ^d
202	P _a ²	Λ	4.253724(2)	4.253857(3)	2.360146(3)	3.673981(5)
	P _b ²	B	0.8235767(2)	0.8033395(5)	0.6623031(6)	0.7823356(4)
	P _c ²	C	0.7925390(3)	0.7737701(5)	0.6426782(7)	0.7328606(4)
	{P _a , P _b }	D _{ab}	-0.004171(4)	-0.004423(5)	-0.00442(2)	0.028047(3)
440	P _γ ⁴	k ₄	-8.985(1)x10 ⁻³	-8.991(1)x10 ⁻³	-9.1296(6)x10 ⁻³	-2.9420(6)x10 ⁻³
	(1-cos6γ)/2	V ₆	-1.60(5)	-1.5785(4)	-1.6731(5)	-1.6001(4)
431	P _γ ³ P _a	k ₃	-3.5072(3)x10 ⁻²	-3.5076(4)x10 ⁻²	-3.6016(3)x10 ⁻²	-1.1183(2)x10 ⁻²
422	P _γ ² P ²	G _v	-1.18853(4)x10 ⁻⁴	-1.13802(6)x10 ⁻⁴	-7.8362(2)x10 ⁻⁵	-8.423(2)x10 ⁻⁵
	P _a ² P _a ²	k ₂	-5.1906(4)x10 ⁻²	-5.1890(5)x10 ⁻²	-5.3409(4)x10 ⁻²	-1.6460(2)x10 ⁻²
	2P _γ ² (P _b ² -P _c ²⁾	c ₁	-1.43(1)x10 ⁻⁴	-1.40(3)x10 ⁻⁴	-1.1(2)x10 ⁻⁴	0.5(1)x10 ⁻⁵
	P _γ ² {P _a , P _b }	Δ _{ab}	1.9(1)x10 ⁻⁴	-0.8(2)x10 ⁻⁴		2.80(9)x10 ⁻⁴
	sin3γ{P _a , P _c }	D _{ac}	1.52(1)x10 ⁻²	1.16(2)x10 ⁻²	0.917(3)x10 ⁻²	1.90(2)x10 ⁻²
	sin3γ{P _b , P _c }	D _{bc}	-1.02(1)x10 ⁻³	-1.02(3)x10 ⁻³	.82)x10 ⁻⁴	1.10(3)x10 ⁻³
	(1-cos3γ)P ²	F _v	-2.38796(8)x10 ⁻³	-2.33063(8)x10 ⁻³	-1.8335(3)x10 ⁻³	-2.22287(9)x10 ⁻³
	(1-cos3γ)P _a ²	k ₅	1.1183(1)x10 ⁻²	1.1160(1)x10 ⁻²	5.811(2)x10 ⁻³	1.2680(5)x10 ⁻²
	(1-cos3γ)(P _b ² -P _c ²⁾	e ₂	-7.60(3)x10 ⁻⁵	-8.09(5)x10 ⁻⁵	6.7(2)x10 ⁻⁵	-1.459(8)x10 ⁻⁴
	(1-cos3γ){P _a , P _b }	d _{ab}	9.048(2)x10 ⁻³	8.879(5)x10 ⁻³	6.80(2)x10 ⁻³	7.805(5)x10 ⁻³
413	P _γ ³ P _a ²	L _v	-1.90289(9)x10 ⁻⁴	-1.8220(1)x10 ⁻⁴	-1.06(8)x10 ⁻⁴	-1.2021(6)x10 ⁻⁴
	P _γ ³ P _a ³	k ₁	-3.459(1)x10 ⁻²	-3.4566(3)x10 ⁻²	-3.475(3)x10 ⁻²	-1.100(2)x10 ⁻²
	P _γ {P _a , (P _b ² -P _c ^{2)}}	c ₄	-1.91(1)x10 ⁻⁴	-1.86(3)x10 ⁻⁴	-1.4(2)x10 ⁻⁴	-0.39(1)x10 ⁻⁴
	P _γ {P _a ² P _b +P _b (P _a ²)}	δ _{ab}	6.6(2)x10 ⁻⁴	0.9(3)x10 ⁻⁴	2.3(3)x10 ⁻⁴	3.1(1)x10 ⁻⁴
404	-P ⁴	Δ _J	1.68627(5)x10 ⁻⁶	1.6238(1)x10 ⁻⁶	0.981(4)x10 ⁻⁶	1.4484(2)x10 ⁻⁶
	-P ² P _a ²	Δ _{JK}	8.480(2)x10 ⁻⁵	8.173(3)x10 ⁻⁵	3.7(7)x10 ⁻⁵	4.786(8)x10 ⁻⁵
	-P _a ⁴	Δ _K	8.77(1)x10 ⁻³	8.7650(5)x10 ⁻³	8.29(3)x10 ⁻³	2.80(1)x10 ⁻³
	-2P ² (P _b ² -P _c ²⁾	δ _J	5.873(2)x10 ⁻⁸	5.57(2)x10 ⁻⁸	2.60(2)x10 ⁻⁸	9.77(3)x10 ⁻⁸
	-{P _a ² , (P _b ² -P _c ^{2)}}	δ _K	5.241(7)x10 ⁻⁵	4.95(3)x10 ⁻⁵	3.34(8)x10 ⁻⁵	4.16(2)x10 ⁻⁵
	{P _a , P _b }P ²	D _{abl}	1.26(6)x10 ⁻⁷		0.5(1)x10 ⁻⁷	-6.47(6)x10 ⁻⁷
	{P _a ² , P _b }	D _{abK}	4.6(1)x10 ⁻⁴	1.54(9)x10 ⁻⁴	2.3(3)x10 ⁻⁴	0.49(4)x10 ⁻⁴
660	(1-cos9γ)/2	V ₉	1.0(2)	1.037(fixed)		
	P _γ ⁶	k _{4B}	1.044(2)x10 ⁻⁵	1.27(2)x10 ⁻⁵	-1.038(9)x10 ⁻⁵	0.15(1)x10 ⁻⁵
651	P _γ ³ P _a	k _{3B}	6.931(7)x10 ⁻⁵	8.06(10)x10 ⁻⁵	-4.67(4)x10 ⁻⁵	1.18(5)x10 ⁻⁵
642	P _γ ⁴ P ²	M _v	8.63(8)x10 ⁻⁸	8.1(1)x10 ⁻⁸	6.8(3)x10 ⁻⁸	-0.9(1)x10 ⁻⁸
	P _γ ⁴ P _a ²	K ₁	1.863(1)x10 ⁻⁴	2.10(2)x10 ⁻⁴	-8.21(7)x10 ⁻⁵	3.46(9)x10 ⁻⁵
	P _γ ³ {P _a , P _b }	ΔΔ _{ab}	2.544x10 ⁻¹⁰ (fixed)	7.054(7)x10 ⁻⁹		
	(1-cos6γ)P ²	N _v	-4.4(3)x10 ⁻⁶	-3.6(3)x10 ⁻⁶	-0.45(6)x10 ⁻⁵	
	(1-cos6γ)P _a ²	K ₂	-1.89(4)x10 ⁻⁴	-2.37(4)x10 ⁻⁴	0.2(3)x10 ⁻⁴	-3.0(1)x10 ⁻⁴
	(1-cos6γ)(P _b ² -P _c ²⁾	c ₁₁	-6.7(3)x10 ⁻⁶	-4.4(5)x10 ⁻⁶	-2.4(4)x10 ⁻⁵	-2.8(1)x10 ⁻⁵
	(1-cos6γ){P _a , P _b }	dd _{ab}	1.55(5)x10 ⁻⁴	2.2(1)x10 ⁻⁴	2.2(2)x10 ⁻⁴	-1.05(9)x10 ⁻⁴
633	P _γ ³ P _a ³	K ₃	2.6183(9)x10 ⁻⁴	2.87(2)x10 ⁻⁴	-6.85(6)x10 ⁻⁵	5.08(8)x10 ⁻⁵
	P _γ ³ P _a ²	k _{3J}	3.30(2)x10 ⁻⁷	3.12(5)x10 ⁻⁷	2.5(1)x10 ⁻⁷	
	P _γ ³ {P _a , (P _b ² -P _c ^{2)}}	c ₁₂	-2.1(8)x10 ⁻⁹	-3.2(3)x10 ⁻⁹		
	P _γ ³ {P _a ² , P _b }	δδ _{ab}	-8.790x10 ⁻¹⁰ (fixed)			
	{(1-cos3γ), P _a ² P _γ }	K _{6J}			-1.2(4)x10 ⁻⁵	
	{(1-cos3γ), P _a ³ P _γ }	K _{6K}	2.02(6)x10 ⁻⁴	2.024x10 ⁻⁴ (fixed)	-2.3(2)x10 ⁻⁴	0.99(9)x10 ⁻⁴
624	P _γ ² P ⁴	g _v	1.13(1)x10 ⁻⁹	1.03(3)x10 ⁻⁹	0.5(1)x10 ⁻⁹	0.40(1)x10 ⁻⁹
	P _γ ² P _a ² P ²	k _{2J}	4.93(2)x10 ⁻⁷	4.55(6)x10 ⁻⁷	3.5(2)x10 ⁻⁷	0.32(3)x10 ⁻⁷
	P _γ ² P _a ⁴	k _{2K}	2.0411(3)x10 ⁻⁴	2.20(1)x10 ⁻⁴	-2.42(2)x10 ⁻⁵	0.404(4)x10 ⁻⁴
	2P _γ ² P ² (P _b ² -P _c ²⁾	e ₅	-5.776x10 ⁻¹³ (fixed)			
	2P _γ ² {P _a ² , (P _b ² -P _c ^{2)}}	e ₈	-0.15(38)x10 ⁻⁹			-1.7(1)x10 ⁻⁸
	(1-cos3γ)P ⁴	f _v	6.27(7)x10 ⁻⁹	5.5(1)x10 ⁻⁹	6.6(5)x10 ⁻⁹	6.4(3)x10 ⁻⁹
	(1-cos3γ)P _a ² P ²	k _{5J}	-5.3(2)x10 ⁻⁷	-2.4(3)x10 ⁻⁷	-2.2(7)x10 ⁻⁵	-0.208(5)x10 ⁻⁵
	(1-cos3γ)P _a ⁴	f _K	3.3(1)x10 ⁻⁴	3.2797(3)x10 ⁻⁴	-4.2(3)x10 ⁻⁴	1.4(1)x10 ⁻⁴
	(1-cos3γ)(P _b ² -P _c ^{2)P²}	e _{2J}		3.5(8)x10 ⁻⁹		0.20(1)x10 ⁻⁷
	(1-cos3γ){P _a ² , (P _b ² -P _c ^{2)}}	e ₉	-1.201x10 ⁻⁸ (fixed)			
615	P _γ ⁵	l _K	8.396x10 ⁻⁵ (fixed)	8.91(4)x10 ⁻⁵		1.67(1)x10 ⁻⁵
	P _γ ³ P _a ²	λ _v	3.51(2)x10 ⁻⁷	2.99(3)x10 ⁻⁷	2.24(8)x10 ⁻⁷	0.26(3)x10 ⁻⁷
	P _γ ³ P _a ⁴	l _v	1.34(1)x10 ⁻⁹	1.18(3)x10 ⁻⁹	0.41(9)x10 ⁻⁹	
	P _γ ³ {P _a , (P _b ² -P _c ^{2)}}	c ₇	6.997x10 ⁻¹¹ (fixed)			
	P _γ ³ {P _a ² , (P _b ² -P _c ^{2)}}	c _{7K}				-0.31(3)x10 ⁻⁷
606	P ⁶	H _J	-1.446x10 ⁻¹² (fixed)		-0.29(4)x10 ⁻¹¹	
	P ⁴ P _a ²	H _{JK}	4.53(6)x10 ⁻¹⁰	4.1(2)x10 ⁻¹⁰	0.8(4)x10 ⁻¹⁰	
	P _a ⁴ P ²	H _{KJ}	1.03(1)x10 ⁻⁷	0.765(7)x10 ⁻⁷	0.59(2)x10 ⁻⁷	0.054(8)x10 ⁻⁷
	P _a ⁶	H _K	1.4264(2)x10 ⁻⁵	1.497(6)x10 ⁻⁵	1.43(2)x10 ⁻⁶	2.83(1)x10 ⁻⁶
	P ² {P _a ² , (P _b ² -P _c ^{2)}}	h _{JK}	8.757x10 ⁻¹¹ (fixed)			

^a Order of the Hamiltonian term in the notation of Ref. 2: n = 1 + m, where n is the total order of the operator, l is the order of the torsional factor, and m is the order of the rotational factor.

^b Notation of Ref. 6. {A,B} = AB + BA. The product of the parameter and operator from a given row yields the term actually used in the vibration-rotation-torsion Hamiltonian, except for F, ρ and A, which occur in the Hamiltonian in the form F(P_γ + ρP_a)² + AP_a².

^c Parameter uncertainties are given in parentheses, and represent one standard deviation in the last digit.

^d ρ is unitless.

TABLE 2
 CH_3OD MW and MMW $v_t = 0 \leftarrow 0$ and $v_t = 1 \leftarrow 1$ Transitions of A Torsional Symmetry for $J \leq 20$,
 with O - C Residuals from the Global Fit

J' P' J'' P''	Freq (MHz)	Unc (kHz)	O-C (kHz)	Ref	J' P' J'' P''	Freq (MHz)	Unc (kHz)	O-C (kHz)	Ref	J' P' J'' P''	Freq (MHz)	Unc (kHz)	O-C (kHz)	Ref
$v_t = 0 \leftarrow 0$ K = 0 \leftarrow 0					$v_t = 0 \leftarrow 0$ K = 1 \leftarrow 2					$v_t = 0 \leftarrow 0$ K = 2 \leftarrow 3				
1 + 0 +	45359.400	100	57	B	8 + 7 +	15720.990	100	-26	B	9 + 8 +	10279.780	100	133	D
2 + 1 +	90705.810	100	49	B	11 + 10 +	126441.169	100	-33	O	12 - 11 -	139625.462	100	129	O
3 + 2 +	136026.400	100	57	A,O	7 - 6 -	15467.910	100	60	B	$v_t = 0 \leftarrow 0$ K = 3 \leftarrow 2				
4 + 3 +	181308.197	100	-14	D	8 - 7 -	66100.090	100	32	B	5 + 6 +	127846.008	100	73	O
5 + 4 +	226538.674	100	81	D	16 - 15 -	491247.684	*	-1402	O	6 + 7 +	82040.930	100	41	B
6 + 5 +	271704.930	100	-4	D	$v_t = 0 \leftarrow 0$ K = 2 \leftarrow 1					7 + 8 +	36018.245	*	-465	D
7 + 6 +	316795.070	100	-11	E	3 + 4 +	146278.639	100	-132	O	3 + 3 -	400575.320	100	93	E
8 + 7 +	361797.570	100	20	E	5 + 6 +	63498.660	100	-1	B	4 + 4 -	400606.860	100	103	E
9 + 8 +	406701.869	100	10	D	6 + 7 +	23407.495	100	29	C,E	5 + 5 -	400676.740	100	43	E
$v_t = 0 \leftarrow 0$ K = 0 \leftarrow 1					2 + 2 -	318790.250	100	-105	E	6 + 6 -	400804.820	100	-10	E
4 + 3 +	52098.820	100	27	B	3 + 3 -	316791.590	100	-75	E	7 + 7 -	401014.290	100	-48	E
6 + 5 +	148359.772	100	-119	D	4 + 4 -	314185.680	100	-96	E	8 + 8 -	401331.420	100	-73	D
7 + 6 +	197233.476	100	-104	D	5 + 5 -	311023.410	100	-32	E	9 + 9 -	401785.240	100	-85	D
9 + 8 +	296158.270	100	-105	E	6 + 6 -	307368.180	100	7	E	3 + 2 +	536618.978	100	87	D
13 + 12 +	496620.093	100	-135	O	7 + 7 -	303296.120	100	28	E	4 + 3 +	581936.701	100	159	D
$v_t = 0 \leftarrow 0$ K = 1 \leftarrow 0					8 + 8 -	298895.680	100	109	E	5 + 4 +	627206.156	100	221	D
1 + 2 +	41859.390	100	23	C	9 + 9 -	294266.750	100	166	E	6 + 5 +	672395.296	*	-531	D
1 - 1 +	133925.423	100	2	D,O	2 + 1 +	412226.183	100	-37	D	5 - 6 -	128675.024	100	-19	O
2 - 2 +	135295.241	100	9	D,O	3 + 2 +	458973.826	100	-59	D	6 - 7 -	83534.600	100	42	B
3 - 3 +	137370.450	100	79	B,O	4 + 3 +	506459.692	100	-35	D	7 - 8 -	38510.100	100	3	B
4 - 4 +	140175.200	100	42	B,O	5 + 4 +	554728.596	100	-39	D	3 - 3 +	400516.340	100	139	E
5 - 5 +	143741.650	100	-4	B,O	6 + 5 +	603837.340	100	42	D	4 - 4 +	400430.210	100	63	E
6 - 6 +	148109.248	100	14	D	7 + 6 +	653853.566	100	-33	D	5 - 5 +	400266.100	100	60	E
7 - 7 +	153323.998	100	71	D	8 + 7 +	704855.718	100	25	D	6 - 6 +	399987.140	100	-17	E
8 - 8 +	159437.464	100	32	D	2 - 3 -	180677.030	100	-15	O	7 - 7 +	399550.610	100	-61	E
9 - 9 +	166505.736	100	-4	D	3 - 4 -	132619.491	100	-48	O	8 - 8 +	398908.530	100	-115	E
1 + 0 +	177924.181	*	-289	D	4 - 5 -	83903.300	100	-62	B	9 - 9 +	398009.240	100	-199	E
2 + 1 +	221920.254	100	0	D	5 - 6 -	34537.320	100	-91	B,E	4 - 3 -	581996.056	*	-328	D
3 + 2 +	265235.846	100	85	D	2 - 2 +	322859.200	100	-66	E	5 - 4 -	627386.150	100	31	D
4 + 3 +	307883.550	*	285	E	3 - 3 +	324893.490	100	0	E	6 - 5 -	672817.983	100	64	D
5 + 4 +	349883.620	100	-16	E	4 - 4 +	327608.560	100	4	E	$v_t = 0 \leftarrow 0$ K = 3 \leftarrow 3				
6 + 5 +	391266.370	100	-65	E	5 - 5 +	331006.540	100	4	E	4 + 3 +	181421.900	*	1457	D
7 + 6 +	432070.130	100	189	D	6 - 6 +	335089.660	100	3	E	5 + 4 +	226776.522	100	19	D
8 + 7 +	472341.086	100	52	D	7 - 7 +	339860.100	100	35	E	6 + 5 +	272132.944	200	297	D
9 + 8 +	512134.795	100	-58	D	8 - 8 +	345319.590	100	31	E	7 + 6 +	317488.752	200	398	D
$v_t = 0 \leftarrow 0$ K = 1 \leftarrow 1					9 - 9 +	351469.260	*	-39	E	8 + 7 +	362842.700	100	-124	E
3 - 3 +	8160.970	100	17	D	2 - 1 -	410854.053	100	-46	D	9 + 8 +	408197.592	*	2651	D
4 - 4 +	13600.040	100	-64	D	3 - 2 -	454833.780	*	-239	D	11 + 10 +	498886.239	*	311	O
5 - 5 +	20396.670	100	59	B	4 - 3 -	498121.391	100	-59	D	4 - 3 -	181421.081	100	26	D
6 - 6 +	28547.810	100	77	B	5 - 4 -	540714.926	100	-88	D	5 - 4 -	226778.738	100	91	D
7 - 7 +	38049.060	100	-8	B	6 - 5 -	582614.701	*	263	D	6 - 5 -	272138.320	100	-43	E
8 - 8 +	48894.000	100	52	B	7 - 6 -	623820.802	100	30	D	7 - 6 -	317501.180	100	-27	E
14 - 14 +	141326.365	*	-1025	O	8 - 7 -	664336.715	100	49	D	8 - 7 -	362868.490	100	-18	E
2 + 1 +	89355.100	100	-27	B	9 - 8 -	704166.879	100	159	D	9 - 8 -	408241.940	100	-34	D
3 + 2 +	134021.283	100	15	D,O	$v_t = 0 \leftarrow 0$ K = 2 \leftarrow 2					$v_t = 0 \leftarrow 0$ K = 3 \leftarrow 4				
4 + 3 +	178673.890	100	43	A	16 + 16 -	33841.064	100	79	W	15 + 14 +	131152.834	100	-112	O
5 + 4 +	223308.567	100	-15	D	3 + 2 +	136102.820	100	28	A	15 - 14 -	133057.284	100	-333	O
6 + 5 +	267921.475	100	83	D	4 + 3 +	181507.140	100	30	A	$v_t = 0 \leftarrow 0$ K = 4 \leftarrow 3				
7 + 6 +	312508.440	100	0	E	5 + 4 +	226942.830	100	75	D	8 + 9 +	140474.632	100	185	O
8 + 7 +	357066.220	100	45	E	6 + 5 +	272417.280	100	35	E	8 - 9 -	140380.006	100	125	O
9 + 8 +	401591.444	100	76	D	7 + 6 +	317937.730	100	37	E	5 + 5 -	548662.947	*	128	D
11 + 10 +	490532.881	100	-110	O	8 + 7 +	363510.600	100	66	E	5 - 5 +	548666.369	*	698	D
2 - 1 -	92075.510	100	-62	B	9 + 8 +	409141.210	100	29	D	6 + 6 -	548657.807	200	156	D
3 - 2 -	138101.530	100	48	A,O	3 - 2 -	136055.460	100	-32	A,O	6 - 6 +	548666.369	200	181	D
4 - 3 -	184113.180	*	182	A	4 - 3 -	181388.970	100	57	A	7 + 7 -	548645.593	200	38	D
5 - 4 -	230105.096	100	7	D	5 - 4 -	226706.601	100	38	D	7 - 7 +	548666.369	*	-474	D
6 - 5 -	276072.520	100	6	E	6 - 5 -	272004.510	100	-3	E	8 + 8 -	548622.407	100	131	D
7 - 6 -	322009.760	100	-14	E	7 - 6 -	317278.870	100	23	E	8 - 8 +	548669.222	100	255	D
8 - 7 -	367911.010	100	-45	E	8 - 7 -	362525.700	100	31	E	9 + 9 -	548581.989	100	77	D
9 - 8 -	413772.286	*	2119	D	9 - 8 -	407741.133	100	24	D	9 - 9 +	548675.146	100	180	D
					11 - 10 -	498062.816	*	236	O					

Note: Refs.: A, (9); B, (10); C, (11); D, (12); E, (13); W, (24); O, new Ohio State FASST measurements.

TABLE 2—Continued

J' P' J'' P''	Freq (MHz)	Unc (kHz)	O-C (kHz)	Ref	J' P' J'' P''	Freq (MHz)	Unc (kHz)	O-C (kHz)	Ref	J' P' J'' P''	Freq (MHz)	Unc (kHz)	O-C (kHz)	Ref
$v_1 = 0 \leftarrow 0$	$K = 4 \leftarrow 4$				$v_1 = 0 \leftarrow 0$	$K = 9 \leftarrow 9$				$v_1 = 1 \leftarrow 1$	$K = 2 \leftarrow 2$			
5 + 4 +	226777.175	100	-259	D	11 + 10 +	498382.778	100	27	O	11 + 10 +	496413.502	*	392	O
5 - 4 -	226777.175	100	-253	D	11 - 10 -	498382.778	100	27	O	3 - 2 -	135663.760	100	8	A.E.O
6 + 5 +	272132.944	200	-251	D	$v_1 = 0 \leftarrow 0$	$K = 10 \leftarrow 10$				4 - 3 -	180875.330	100	-38	A.E
6 - 5 -	272132.944	200	-220	D	11 + 10 +	498249.264	100	-30	O	5 - 4 -	226078.570	100	-92	E
7 + 6 +	317488.752	200	-359	D	11 - 10 -	498249.264	100	-30	O	6 - 5 -	271271.340	100	-135	E
7 - 6 -	317488.752	200	-258	D	$v_1 = 1 \leftarrow 0$	$K = 5 \leftarrow 9$				7 - 6 -	316451.490	100	-113	E
8 + 7 +	362845.108	100	-120	D	19 + 20 +	128970.191	*	-404	O	8 - 7 -	361616.670	100	-127	E
8 - 7 -	362845.108	100	160	D	19 - 20 -	128970.191	*	-493	O	11 - 10 -	496999.484	100	-64	O
11 + 10 +	498916.041	100	-417	O	$v_1 = 1 \leftarrow 1$	$K = 0 \leftarrow 0$				$v_1 = 1 \leftarrow 1$	$K = 2 \leftarrow 3$			
11 - 10 -	498912.932	100	208	O	1 + 0 +	45266.320	100	23	B	18 + 17 +	30470.987	100	115	W
$v_1 = 0 \leftarrow 0$	$K = 5 \leftarrow 4$				2 + 1 +	90534.530	100	-69	B	$v_1 = 1 \leftarrow 1$	$K = 3 \leftarrow 2$			
6 + 7 +	489558.696	100	-270	O	3 + 2 +	135806.920	100	5	A.E.O	13 + 14 +	128123.432	100	-328	O
6 - 7 -	489558.696	100	-410	O	4 + 3 +	181085.210	100	-52	A.E	$v_1 = 1 \leftarrow 1$	$K = 3 \leftarrow 3$			
16 + 17 +	34329.994	100	-399	W	5 + 4 +	226371.540	100	-123	E	4 + 3 +	181046.090	*	339	A
16 - 17 -	34502.157	100	496	W	6 + 5 +	271668.040	100	-103	E	5 + 4 +	226331.800	100	-56	E
$v_1 = 0 \leftarrow 0$	$K = 5 \leftarrow 5$				7 + 6 +	316976.560	100	-164	E	6 + 5 +	271633.590	100	-70	E
6 + 5 +	272094.810	100	-7	E	8 + 7 +	362299.210	100	-199	E	7 + 6 +	316953.460	100	-66	E
6 - 5 -	272094.810	100	-7	E	$v_1 = 1 \leftarrow 1$	$K = 0 \leftarrow 1$				8 + 7 +	362293.120	100	-240	E
7 + 6 +	317438.880	100	28	E	2 + 3 +	494084.922	*	-926	O	$v_1 = 1 \leftarrow 1$	$K = 3 \leftarrow 3$			
7 - 6 -	317438.880	100	27	E	$v_1 = 1 \leftarrow 1$	$K = 1 \leftarrow 0$				4 - 3 -	181046.090	*	-320	A
8 + 7 +	362780.480	100	-38	E	16 + 15 +	34546.913	100	26	W	5 - 4 -	226334.090	100	-70	E
8 - 7 -	362780.480	100	-39	E	19 + 18 +	134259.661	*	-8406	O	6 - 5 -	271639.710	100	-82	E
9 + 8 +	408119.471	100	9	D	$v_1 = 1 \leftarrow 1$	$K = 1 \leftarrow 1$				7 - 6 -	316967.220	100	-65	E
9 - 8 -	408119.471	100	6	D	2 + 1 +	89961.380	100	167	D.E	8 - 7 -	362320.730	100	-39	E
11 + 10 +	498788.129	100	373	O	3 + 2 +	134925.646	100	286	E.O	11 - 10 -	498579.934	100	214	O
11 - 10 -	498788.129	100	350	O	4 + 3 +	179870.330	100	408	E	$v_1 = 1 \leftarrow 1$	$K = 4 \leftarrow 4$			
$v_1 = 0 \leftarrow 0$	$K = 6 \leftarrow 5$				5 + 4 +	224789.070	100	418	E	11 + 10 +	497234.321	200	-194	O
11 + 12 +	484868.607	100	80	O	6 + 5 +	269676.030	100	466	E	11 - 10 -	497234.321	200	186	O
11 - 12 -	484868.607	100	170	O	7 + 6 +	314525.440	100	431	E	$v_1 = 1 \leftarrow 1$	$K = 4 \leftarrow 5$			
$v_1 = 0 \leftarrow 0$	$K = 6 \leftarrow 6$				8 + 7 +	359332.150	100	379	E	20 + 19 +	491361.569	*	-2320	O
7 + 6 +	317357.216	100	36	D	11 + 10 +	493452.312	100	92	O	20 - 19 -	491276.963	*	-7108	O
7 - 6 -	317357.216	100	36	D	2 - 1 -	91120.780	100	1	D.E	$v_1 = 1 \leftarrow 1$	$K = 5 \leftarrow 4$			
8 + 7 +	362678.588	100	73	D	3 - 2 -	136663.960	100	-50	E.O	8 + 9 +	32315.301	100	-206	W
8 - 7 -	362678.588	100	73	D	4 - 3 -	182186.480	100	-78	E	8 - 9 -	32315.301	100	-349	W
9 + 8 +	407993.723	100	47	D	5 - 4 -	227681.290	100	-93	E	$v_1 = 1 \leftarrow 1$	$K = 5 \leftarrow 5$			
9 - 8 -	407993.723	100	47	D	6 - 5 -	273141.100	100	-233	E	11 + 10 +	495222.400	100	-287	O
11 + 10 +	498602.490	100	140	O	7 - 6 -	318559.060	100	-85	E	11 - 10 -	495222.400	100	-287	O
11 - 10 -	498602.490	100	141	O	8 - 7 -	363927.430	100	-25	E	$v_1 = 1 \leftarrow 1$	$K = 6 \leftarrow 6$			
$v_1 = 0 \leftarrow 0$	$K = 7 \leftarrow 6$				$v_1 = 1 \leftarrow 1$	$K = 1 \leftarrow 2$				11 + 10 +	498934.109	100	405	O
13 + 14 +	492605.236	100	-94	O	2 + 3 +	143617.400	100	204	O	11 - 10 -	498934.109	100	406	O
13 - 14 -	492605.236	100	-97	O	2 - 3 -	145342.681	100	-215	O	$v_1 = 1 \leftarrow 1$	$K = 7 \leftarrow 7$			
$v_1 = 0 \leftarrow 0$	$K = 7 \leftarrow 7$				$v_1 = 1 \leftarrow 1$	$K = 2 \leftarrow 1$				11 + 10 +	497809.362	100	94	O
8 + 7 +	362584.265	100	-119	D	7 - 6 -	29661.170	*	240	W	11 - 10 -	497809.362	100	94	O
8 - 7 -	362584.265	100	-119	D	9 + 8 +	135440.150	*	-3107	O	$v_1 = 1 \leftarrow 1$	$K = 8 \leftarrow 8$			
9 + 8 +	407880.723	100	-94	D	18 - 17 -	498839.328	*	-5098	O	11 + 10 +	497342.771	100	5	O
9 - 8 -	407880.723	100	-94	D	$v_1 = 1 \leftarrow 1$	$K = 2 \leftarrow 2$				11 - 10 -	497342.771	100	5	O
11 + 10 +	498444.040	100	-417	O	3 + 2 +	135652.720	100	-19	A.E	$v_1 = 1 \leftarrow 1$	$K = 9 \leftarrow 9$			
11 - 10 -	498444.040	100	-417	O	4 + 3 +	180847.820	100	-68	A.E	11 + 10 +	495207.162	100	189	O
$v_1 = 0 \leftarrow 0$	$K = 8 \leftarrow 8$				5 + 4 +	226023.710	100	-128	E	11 - 10 -	495207.162	100	189	O
11 + 10 +	498411.117	100	19	O	6 + 5 +	271175.720	100	-105	E	$v_1 = 1 \leftarrow 1$	$K = 10 \leftarrow 10$			
11 - 10 -	498411.117	100	19	O	7 + 6 +	316299.050	100	-71	E	11 + 10 +	497194.431	100	-187	O
					8 + 7 +	361389.060	100	9	E	11 - 10 -	497194.431	100	-187	O

and strong downward shifts of the $K = 0$ and -1 levels at high J are quite striking.

To explore qualitatively the effects of asymmetry mixing in producing this energy pattern, we used Matlab to set up and diagonalize a simple 5×5 Hamiltonian matrix for the $K = 0$ to $\pm 2 E$ levels of given J . We took the $J = 2$ Ritz term values as the unperturbed diagonal elements and used molecular constants $D_{ab} = 840.8$ MHz and $(B - C) = 1483.2$ MHz derived from Table 1 to calculate the $\Delta K = \pm 1$ and $\Delta K = \pm 2$

off-diagonal asymmetry matrix elements. Figure 1b illustrates the resulting energy curves, showing the $K = 0$ and -1 energies slowly converging to a minimum separation at $J = 16$ and then gradually moving apart again at higher J . The experimental and calculated patterns are remarkably similar, showing that asymmetry coupling is certainly the dominant contributor to the energy perturbations. However, in quantitative detail the separation between $K = 0$ and -1 levels calculated from the simple 5×5 model is significantly larger than that

TABLE 3
CH₃OD MW and MMW $v_t = 0 \leftarrow 0$ and $v_t = 1 \leftarrow 1$ Transitions of E Torsional Symmetry for $J \leq 20$,
with O - C Residuals from the Global Fit

J'	J''	Freq (MHz)	Unc (kHz)	O-C (kHz)	Ref	J'	J''	Freq (MHz)	Unc (kHz)	O-C (kHz)	Ref	J'	J''	Freq (MHz)	Unc (kHz)	O-C (kHz)	Ref
$v_t = 0 \leftarrow 0$ K = -10 \leftarrow -10						$v_t = 0 \leftarrow 0$ K = -3 \leftarrow -2						$v_t = 0 \leftarrow 0$ K = -1 \leftarrow -0					
11	10	498252.761	100	-20	O	10	10	485879.205	*	249	O	10	10	14585.770	100	-74	L
$v_t = 0 \leftarrow 0$ K = -9 \leftarrow -9						$v_t = 0 \leftarrow 0$ K = -2 \leftarrow -3						$v_t = 0 \leftarrow 0$ K = -1 \leftarrow -1					
11	10	498267.732	100	-292	O	11	11	484119.419	*	657	O	11	11	13027.540	*	585	L
$v_t = 0 \leftarrow 0$ K = -8 \leftarrow -8						$v_t = 0 \leftarrow 0$ K = -2 \leftarrow -2						$v_t = 0 \leftarrow 0$ K = 0 \leftarrow -1					
11	10	498371.001	100	67	O	14	13	127983.895	100	148	O	12	12	11357.550	100	350	L
$v_t = 0 \leftarrow 0$ K = -7 \leftarrow -7						$v_t = 0 \leftarrow 0$ K = -2 \leftarrow -1						$v_t = 0 \leftarrow 0$ K = 0 \leftarrow -0					
8	7	362644.680	100	30	D	3	2	136107.600	100	-22	A,O	1	0	64302.160	100	156	B
9	8	407954.920	100	5	D	4	3	181504.500	100	58	A	2	1	109662.000	*	546	O
$v_t = 0 \leftarrow 0$ K = -6 \leftarrow -6						$v_t = 0 \leftarrow 0$ K = -2 \leftarrow -0						$v_t = 0 \leftarrow 0$ K = 0 \leftarrow -0					
7	6	317393.226	*	504	D	5	4	226922.584	100	-10	D	3	2	154963.980	100	-45	E
8	7	362722.120	100	-8	D	6	5	272362.153	100	1	D	4	3	200148.144	100	-320	D
9	8	408046.577	100	22	D	7	6	317816.191	100	11	D	5	4	245142.988	100	-160	D
11	10	498678.014	100	74	O	8	7	363266.521	100	12	D	6	5	289871.927	100	-248	D
$v_t = 0 \leftarrow 0$ K = -6 \leftarrow -5						$v_t = 0 \leftarrow 0$ K = -2 \leftarrow -1						$v_t = 0 \leftarrow 0$ K = 0 \leftarrow -1					
9	10	486614.917	100	-323	O	2	3	133375.340	100	-77	O	2	1	71711.910	100	-120	B
19	20	33638.661	100	-190	W	3	4	88340.240	100	25	B	4	3	162185.730	100	102	E
$v_t = 0 \leftarrow 0$ K = -5 \leftarrow -5						$v_t = 0 \leftarrow 0$ K = -1 \leftarrow -2						$v_t = 0 \leftarrow 0$ K = 0 \leftarrow -1					
6	5	272073.637	100	-28	D	2	2	269347.820	100	-10	D	5	4	207393.090	100	130	D
7	6	317409.338	100	-65	D	3	3	269483.062	100	23	D	6	5	252624.442	100	124	D
8	7	362740.536	100	-48	D	4	4	269844.680	100	24	D	7	6	297921.374	100	28	D
9	8	408066.462	100	-96	D	5	5	270581.390	100	91	D	8	7	343323.714	100	225	D
11	10	498700.219	100	-81	O	6	6	271864.383	100	115	D	9	8	388857.485	100	131	D
$v_t = 0 \leftarrow 0$ K = -5 \leftarrow -4						$v_t = 0 \leftarrow 0$ K = -1 \leftarrow -1						$v_t = 0 \leftarrow 0$ K = 0 \leftarrow -1					
12	13	127892.656	100	103	O	8	8	276756.291	100	129	D	1	0	45344.160	100	-32	B
14	15	37202.222	100	166	W	9	9	280630.770	100	130	D	2	1	90669.980	100	137	B
$v_t = 0 \leftarrow 0$ K = -4 \leftarrow -5						$v_t = 0 \leftarrow 0$ K = -1 \leftarrow -1						$v_t = 0 \leftarrow 0$ K = 0 \leftarrow -1					
19	18	144238.270	*	-395	O	2	1	360051.423	100	-49	D	3	2	135958.380	100	-5	A,O
$v_t = 0 \leftarrow 0$ K = -4 \leftarrow -4						$v_t = 0 \leftarrow 0$ K = -1 \leftarrow -1						$v_t = 0 \leftarrow 0$ K = 0 \leftarrow -1					
5	4	226738.864	100	-66	D	3	2	405455.439	100	-13	D	4	3	181191.270	100	2	A
6	5	272080.639	100	19	D	4	3	450987.450	100	-30	D	5	4	226350.191	100	35	D
7	6	317418.981	100	-7	D	5	4	496767.286	100	35	D,O	6	5	271417.352	100	42	D
8	7	362753.467	100	-20	D	6	5	542943.610	100	159	D	7	6	316376.222	100	11	D
9	8	408083.545	100	-28	D	7	6	589680.755	*	307	D	8	7	361212.370	100	-24	D
11	10	498728.350	100	-18	O	8	7	637136.727	100	21	D	9	8	405914.393	100	-16	D
$v_t = 0 \leftarrow 0$ K = -4 \leftarrow -3						$v_t = 0 \leftarrow 0$ K = -2 \leftarrow -1						$v_t = 0 \leftarrow 0$ K = 0 \leftarrow -1					
4	5	392720.888	100	125	D	7	6	494779.637	*	-4149	O	11	10	494890.674	100	89	O
5	6	347308.432	100	152	D	$v_t = 0 \leftarrow 0$ K = -1 \leftarrow -2						$v_t = 0 \leftarrow 0$ K = 0 \leftarrow -1					
12	13	28306.763	100	-90	W	7	6	43945.920	100	-63	B	3	2	25695.840	100	52	B
$v_t = 0 \leftarrow 0$ K = -3 \leftarrow -3						$v_t = 0 \leftarrow 0$ K = -1 \leftarrow -1						$v_t = 0 \leftarrow 0$ K = 0 \leftarrow -1					
4	3	181428.240	100	122	A	8	7	86510.220	100	-127	B	4	3	70715.450	100	35	D,E
5	4	226788.612	100	1	D	9	8	128049.376	100	-153	O	6	5	159571.090	100	65	E
6	5	272151.453	100	40	D	$v_t = 0 \leftarrow 0$ K = -1 \leftarrow -1						$v_t = 0 \leftarrow 0$ K = 0 \leftarrow -1					
7	6	317517.028	100	36	D	2	1	90703.650	100	9	B	7	6	203024.708	100	24	D
8	7	362885.847	100	18	D	3	2	135972.500	100	86	A,O	8	7	245538.036	100	-20	D
9	8	408258.453	100	26	D	4	3	181142.850	100	26	A	9	8	286887.736	*	-860	D
$v_t = 0 \leftarrow 0$ K = -3 \leftarrow -2						$v_t = 0 \leftarrow 0$ K = -1 \leftarrow -1						$v_t = 0 \leftarrow 0$ K = 1 \leftarrow -2					
3	4	325954.609	100	-131	D	5	4	226185.930	100	-22	D	7	6	141731.456	100	39	O
4	5	280460.396	100	133	D	6	5	271079.186	100	3	D	$v_t = 0 \leftarrow 0$ K = 1 \leftarrow -1					
5	6	234886.652	100	-69	D	7	6	315810.235	100	-16	D	12	12	134834.590	100	-134	O
6	7	189221.747	100	-207	D	8	7	360380.551	100	7	D	$v_t = 0 \leftarrow 0$ K = 1 \leftarrow -0					
7	8	143472.330	100	-108	D,O	9	8	404805.709	100	18	D	1	2	19518.790	100	-254	B
3	3	507459.040	100	-141	D	11	10	493331.764	100	68	O	1	1	110188.860	100	-27	A
4	4	507382.760	100	-97	D	$v_t = 0 \leftarrow 0$ K = -1 \leftarrow -0						2	2	110262.640	100	44	A
5	5	507248.796	100	-77	D	1	1	18957.950	100	138	D	3	3	110475.760	100	-94	A
6	6	507038.075	100	-60	D	2	2	18991.670	100	59	D	4	4	110950.750	100	-10	A
7	7	506738.887	100	-59	D	3	3	19005.640	100	0	D	5	5	111846.300	100	15	A
8	8	506358.298	100	32	D	4	4	18957.170	100	-26	D	6	6	113350.800	*	-727	A
9	9	505936.551	100	26	D	5	5	18792.970	100	-22	D	7	7	115674.450	100	112	A
						6	6	18454.760	100	-105	D	8	8	119025.800	100	-13	A
						7	7	17889.040	100	135	C,D	10	10	129575.616	100	-59	O
						8	8	17057.090	100	35	C,D	11	11	137074.525	100	-119	O
						9	9	15948.140	100	-196	L	12	12	146191.998	100	73	O

Note: Refs.: A, (9); B, (10); C, (11); D, (12); E, (13); W, (24); L, (26); O, new Ohio State FASSST measurements.

TABLE 3—Continued

J'	J''	Freq (MHz)	Unc (kHz)	O-C (kHz)	Ref	J'	J''	Freq (MHz)	Unc (kHz)	O-C (kHz)	Ref	J'	J''	Freq (MHz)	Unc (kHz)	O-C (kHz)	Ref																		
$v_i = 0 \leftarrow 0$						$K = 1 \leftarrow 0$						$v_i = 0 \leftarrow 0$						$K = 3 \leftarrow 3$						$v_i = 1 \leftarrow 1$						$K = -5 \leftarrow -5$					
1	0	155533.080	100	2	D	4	3	181451.290	100	41	A	11	10	497597.866	100	17	O	$K = -4 \leftarrow -3$																	
2	1	200932.393	100	-46	D	5	4	226825.536	100	123	D	8	9	144063.623	100	764	O	$K = -3 \leftarrow -2$																	
3	2	246434.165	100	-73	D	6	5	272207.126	100	-6	D	16	16	597080.314	*	1220	O	$K = -2 \leftarrow -1$																	
4	3	292141.956	100	-73	D	7	6	317597.904	100	1	D	13	12	20488.778	100	511	W	$K = -1 \leftarrow 0$																	
5	4	338196.424	100	-17	D	8	7	362999.237	100	12	D	16	15	132590.074	*	-1319	O	$K = 0 \leftarrow 0$																	
6	5	384768.910	100	73	D	9	8	408412.611	100	22	D	4	3	180682.890	100	-35	O	$K = -1 \leftarrow -1$																	
7	6	432050.514	100	-36	D	$v_i = 0 \leftarrow 0$						$K = 4 \leftarrow 3$						$K = -2 \leftarrow -2$																	
8	7	480238.132	100	-75	D	4	5	440339.804	100	-85	D	4	3	180682.890	100	-35	O	$K = -1 \leftarrow -1$																	
9	8	529517.557	100	-126	D	5	6	394901.707	*	-546	D	11	10	495942.890	100	-105	O	$K = -2 \leftarrow -2$																	
$v_i = 0 \leftarrow 0$						$K = 1 \leftarrow 1$						$v_i = 0 \leftarrow 0$						$K = 4 \leftarrow 4$						$v_i = 1 \leftarrow 1$						$K = -3 \leftarrow -3$					
2	1	90743.560	100	8	B	7	8	303904.827	100	-102	D	3	4	181268.200	100	-13	O	$K = -2 \leftarrow -2$																	
3	2	136171.610	100	-32	A,O	8	9	258322.261	100	-64	D	4	5	136578.249	100	98	O	$K = -1 \leftarrow -1$																	
4	3	181666.310	100	135	A	13	14	28977.864	100	327	W	11	10	131759.259	*	-494	O	$K = 0 \leftarrow 0$																	
5	4	227245.714	100	33	D	$v_i = 0 \leftarrow 0$						$K = 4 \leftarrow 4$						$v_i = 1 \leftarrow 1$						$K = -1 \leftarrow -1$											
6	5	272922.588	100	36	D	5	4	226769.541	100	46	D	3	4	181268.200	100	-13	O	$K = 0 \leftarrow 0$																	
7	6	318699.038	100	15	D	6	5	272123.154	100	6	D	4	5	136578.249	100	98	O	$K = -1 \leftarrow -1$																	
8	7	364563.868	100	-1	D	7	6	317476.689	100	33	D	3	2	135894.260	100	135	A,E,O	$K = -2 \leftarrow -2$																	
9	8	410491.860	100	-9	D	8	7	362830.003	100	18	D	4	3	181126.400	100	171	A,E	$K = -3 \leftarrow -3$																	
$v_i = 0 \leftarrow 0$						$K = 1 \leftarrow 2$						$v_i = 0 \leftarrow 0$						$K = 4 \leftarrow 5$						$v_i = 1 \leftarrow 1$						$K = -2 \leftarrow -2$					
5	4	30839.200	100	33	B	9	8	408183.172	100	73	D	5	4	226302.280	100	91	E	$K = -1 \leftarrow -1$																	
6	5	76868.830	100	103	B	11	10	498889.143	*	631	O	6	5	271408.930	100	60	E	$K = 0 \leftarrow 0$																	
$v_i = 0 \leftarrow 0$						$K = 2 \leftarrow 1$						$v_i = 0 \leftarrow 0$						$K = 4 \leftarrow 5$						$v_i = 1 \leftarrow 1$						$K = -1 \leftarrow -1$					
2	3	60487.650	100	28	B	19	18	31501.743	100	-39	W	7	6	316434.450	100	63	E	$K = 0 \leftarrow 0$																	
3	4	14920.430	100	35	B	$v_i = 0 \leftarrow 0$						$K = 5 \leftarrow 5$						$v_i = 1 \leftarrow 1$						$K = -2 \leftarrow -2$											
2	2	196659.300	100	36	D,E	6	5	272052.144	100	34	D	2	2	143624.085	100	-109	O	$K = -1 \leftarrow -1$																	
3	3	196586.601	100	31	D,E	7	6	317383.010	100	30	D	3	3	143758.233	100	-48	O	$K = 0 \leftarrow 0$																	
4	4	196406.501	100	-13	D,E	8	7	362708.696	100	-4	D	4	4	143853.912	100	43	O	$K = -1 \leftarrow -1$																	
5	5	196053.733	100	-92	D	9	8	408028.569	100	38	D	5	5	143840.340	100	142	O	$K = -2 \leftarrow -2$																	
6	6	195459.860	100	-78	D	11	10	498647.507	100	-62	O	6	6	143630.207	100	215	O	$K = -3 \leftarrow -3$																	
7	7	194568.609	100	-155	D	$v_i = 0 \leftarrow 0$						$K = 6 \leftarrow 5$						$v_i = 1 \leftarrow 1$						$K = -4 \leftarrow -4$											
8	8	193358.934	100	-201	D	16	17	141493.019	100	77	O	7	7	143121.231	100	273	O	$K = -5 \leftarrow -5$																	
9	9	191870.147	100	-190	D	$v_i = 0 \leftarrow 0$						$K = 6 \leftarrow 6$						$v_i = 1 \leftarrow 1$						$K = -6 \leftarrow -6$											
3	2	332758.272	100	60	D	7	6	317339.138	100	-103	D	8	8	142198.401	100	174	O	$K = -7 \leftarrow -7$																	
4	3	378072.681	100	-8	D	8	7	362654.326	100	-108	D	9	9	140738.177	100	251	O	$K = -8 \leftarrow -8$																	
5	4	423299.457	100	-49	D	9	8	407961.943	100	-95	D	10	10	138612.032	100	107	O	$K = -9 \leftarrow -9$																	
6	5	468382.407	100	-83	D	11	10	498550.883	*	177	O	11	11	135693.582	100	-7	O	$K = -10 \leftarrow -10$																	
7	6	513267.644	100	-142	D	$v_i = 0 \leftarrow 0$						$K = 7 \leftarrow 6$						$v_i = 1 \leftarrow 1$						$K = -11 \leftarrow -11$											
8	7	557922.635	100	-369	D	12	13	491310.946	100	-106	O	12	12	131863.800	100	-319	O	$K = -12 \leftarrow -12$																	
9	8	602361.855	100	-352	D	$v_i = 0 \leftarrow 0$						$K = 7 \leftarrow 7$						$v_i = 1 \leftarrow 1$						$K = -13 \leftarrow -13$											
$v_i = 0 \leftarrow 0$						$K = 2 \leftarrow 2$						$v_i = 0 \leftarrow 0$						$K = 8 \leftarrow 7$						$v_i = 1 \leftarrow 1$						$K = -14 \leftarrow -14$					
3	2	136098.960	100	12	A	8	7	362649.659	100	-80	D	14	15	489036.673	*	3990	O	$K = -15 \leftarrow -15$																	
4	3	181486.110	100	-9	A	9	8	407958.433	100	-79	D	2	3	136500.513	*	-2730	O	$K = -16 \leftarrow -16$																	
5	4	226892.864	100	-128	D	11	10	498550.883	*	-511	O	$v_i = 0 \leftarrow 0$						$K = 9 \leftarrow 8$						$v_i = 1 \leftarrow 1$						$K = -17 \leftarrow -17$					
6	5	272328.588	100	-77	D	$v_i = 0 \leftarrow 0$						$K = 8 \leftarrow 8$						$v_i = 1 \leftarrow 1$						$K = -18 \leftarrow -18$											
7	6	317807.822	100	-26	D	9	8	407900.892	100	-29	D	17	16	27027.216	*	-1724	W	$K = -19 \leftarrow -19$																	
8	7	363354.205	100	-35	D	11	10	498482.365	100	118	O	$v_i = 0 \leftarrow 0$						$K = 9 \leftarrow 9$						$v_i = 1 \leftarrow 1$						$K = -20 \leftarrow -20$					
9	8	409003.044	100	-28	D	$v_i = 0 \leftarrow 0$						$K = 10 \leftarrow 10$						$v_i = 1 \leftarrow 1$						$K = -21 \leftarrow -21$											
$v_i = 0 \leftarrow 0$						$K = 3 \leftarrow 0$						$v_i = 0 \leftarrow 0$						$K = 10 \leftarrow 10$						$v_i = 1 \leftarrow 1$						$K = -22 \leftarrow -22$					
4	4	484004.999	*	-2084	O	11	10	498138.380	100	-32	O	$v_i = 0 \leftarrow 0$						$K = 10 \leftarrow 10$						$v_i = 1 \leftarrow 1$						$K = -23 \leftarrow -23$					
$v_i = 0 \leftarrow 0$						$K = 3 \leftarrow 2$						$v_i = 0 \leftarrow 0$						$K = 10 \leftarrow 10$						$v_i = 1 \leftarrow 1$						$K = -24 \leftarrow -24$					
5	6	130603.793	100	72	O	11	10	497416.562	100	306	O	$v_i = 0 \leftarrow 0$						$K = 10 \leftarrow 10$						$v_i = 1 \leftarrow 1$						$K = -25 \leftarrow -25$					
6	7	85003.120	100	115	B	$v_i = 1 \leftarrow 1$						$K = -8 \leftarrow -8$						$v_i = 1 \leftarrow 1$						$K = -26 \leftarrow -26$											
7	8	39246.810	100	142	B	11	10	497879.779	100	-131	O	$v_i = 1 \leftarrow 1$						$K = -8 \leftarrow -8$						$v_i = 1 \leftarrow 1$						$K = -27 \leftarrow -27$					
3	3	403034.826	100	-9	D	$v_i = 1 \leftarrow 1$						$K = -7 \leftarrow -7$						$v_i = 1 \leftarrow 1$						$K = -28 \leftarrow -28$											
4	4	402999.945	100	-20	D	11	10	497951.349	100	68	O	$v_i = 1 \leftarrow 1$						$K = -7 \leftarrow -7$						$v_i = 1 \leftarrow 1$						$K = -29 \leftarrow -29$					
5	5	402932.427	100	41	D	$v_i = 1 \leftarrow 1$						$K = -6 \leftarrow -6$						$v_i = 1 \leftarrow 1$						$K = -30 \leftarrow -30$											
6	6	402810.935	100	82	D	10	9	146316.908	*	584	O	$v_i = 1 \leftarrow 1$						$K = -6 \leftarrow -6$						$v_i = 1 \leftarrow 1$						$K = -31 \leftarrow -31$					
7	7	402601.019	100	111	D	$v_i = 1 \leftarrow 1$						$K = -6 \leftarrow -6$						$v_i = 1 \leftarrow 1$						$K = -32 \leftarrow -32$											
8	8	402245.978	100	85	D	11	10	495353.011	100	-192	O	$v_i = 1 \leftarrow 1$						$K = -6 \leftarrow -6$						$v_i = 1 \leftarrow 1$						$K = -33 \leftarrow -33$					
9	9	401655.537	100	127	D	$v_i = 1 \leftarrow 1$						$K = -6 \leftarrow -6$						$v_i = 1 \leftarrow 1$						$K = -34 \leftarrow -34$											
$v_i = 1 \leftarrow 1$						$K = 3 \leftarrow 3$						$v_i = 1 \leftarrow 1$						$K = 10 \leftarrow 10$						$v_i = 1 \leftarrow 1$						$K = -35 \leftarrow -35$					
4	3	181451.290	100	41	A	17	18	490649.483	100	14	O	$v_i = 1 \leftarrow 1$						$K = 10 \leftarrow 10$						$v_i = 1 \leftarrow 1$						$K = -36 \leftarrow -36$					

TABLE 3—Continued

J'	J''	Freq (MHz)	Unc (kHz)	O-C (kHz)	Ref	J'	J''	Freq (MHz)	Unc (kHz)	O-C (kHz)	Ref	J'	J''	Freq (MHz)	Unc (kHz)	O-C (kHz)	Ref																		
$v_i = 1 \leftarrow 1$						$K = 0 \leftarrow 0$						$v_i = 1 \leftarrow 1$						$K = 2 \leftarrow -3$						$v_i = 1 \leftarrow 1$						$K = 4 \leftarrow 5$					
1	0	45260.020	100	126	B	18	18	127439.516	100	105	O	11	10	127165.976	*	-1994	O	11	10	495773.436	100	19	O	11	10	496901.443	*	-548	O	11	10	497690.329	*	-770	O
2	1	90514.920	100	14	B	$v_i = 1 \leftarrow 1$						$K = 2 \leftarrow 1$						$v_i = 1 \leftarrow 1$						$K = 6 \leftarrow 6$											
3	2	135760.133	100	-26	A,O	8	9	496972.281	*	-967	O	11	10	495773.436	100	19	O	11	10	495773.436	100	19	O	11	10	495773.436	100	19	O	11	10	495773.436	100	19	O
4	3	180990.810	100	28	E	19	20	31397.096	100	98	W	$v_i = 1 \leftarrow 1$						$K = 7 \leftarrow 7$																	
5	4	226201.950	100	28	E	$v_i = 1 \leftarrow 1$						$K = 2 \leftarrow 2$						$v_i = 1 \leftarrow 1$						$K = 7 \leftarrow 8$											
6	5	271388.810	100	63	E	3	2	135764.850	100	-65	A,E,O	20	19	142212.347	*	-21954	O	20	19	142212.347	*	-21954	O	20	19	142212.347	*	-21954	O	20	19	142212.347	*	-21954	O
7	6	316546.500	100	37	E	4	3	181024.220	100	28	A,E	13	14	139705.573	*	4792	O	13	14	139705.573	*	4792	O	13	14	139705.573	*	4792	O	13	14	139705.573	*	4792	O
8	7	361670.360	100	29	E	5	4	226287.060	100	-80	E	$v_i = 1 \leftarrow 1$						$K = 8 \leftarrow 7$																	
11	10	496792.856	100	99	O	6	5	271554.570	100	-68	E	11	10	496901.443	*	-548	O	11	10	496901.443	*	-548	O	11	10	496901.443	*	-548	O	11	10	496901.443	*	-548	O
$v_i = 1 \leftarrow 1$						$K = 0 \leftarrow 1$						$v_i = 1 \leftarrow 1$						$K = 8 \leftarrow 8$																	
1	2	11787.620	100	241	L	8	7	362106.500	100	-87	E	11	10	495851.957	*	488	O	11	10	495851.957	*	488	O	11	10	495851.957	*	488	O	11	10	495851.957	*	488	O
$v_i = 1 \leftarrow 1$						$K = 1 \leftarrow 0$						$v_i = 1 \leftarrow 1$						$K = 9 \leftarrow 8$																	
3	2	33419.126	100	-70	W	11	10	497987.167	100	258	O	15	16	136086.988	*	-5466	O	15	16	136086.988	*	-5466	O	15	16	136086.988	*	-5466	O	15	16	136086.988	*	-5466	O
13	12	484471.734	*	-1310	O	11	10	495868.651	100	-244	O	$v_i = 1 \leftarrow 1$						$K = 9 \leftarrow 9$																	
$v_i = 1 \leftarrow 1$						$K = 1 \leftarrow 1$						$v_i = 1 \leftarrow 1$						$K = 4 \leftarrow 3$						$v_i = 1 \leftarrow 1$						$K = 9 \leftarrow 9$					
2	1	90487.270	100	-78	B	5	4	30631.414	100	140	W	11	10	497690.329	*	-770	O	11	10	497690.329	*	-770	O	11	10	497690.329	*	-770	O	11	10	497690.329	*	-770	O
3	2	135721.430	100	-51	E,O	$v_i = 1 \leftarrow 1$						$K = 4 \leftarrow 4$						$v_i = 1 \leftarrow 1$						$K = 4 \leftarrow 4$											
4	3	180944.090	100	-76	E	5	4	225300.080	100	36	E	5	4	225300.080	100	36	E	5	4	225300.080	100	36	E	5	4	225300.080	100	36	E	5	4	225300.080	100	36	E
5	4	226151.520	100	-70	E	6	5	270373.220	100	42	E	6	5	270373.220	100	42	E	6	5	270373.220	100	42	E	6	5	270373.220	100	42	E	6	5	270373.220	100	42	E
6	5	271339.880	100	-63	E	7	6	315450.750	100	44	E	7	6	315450.750	100	44	E	7	6	315450.750	100	44	E	7	6	315450.750	100	44	E	7	6	315450.750	100	44	E
7	6	316505.350	100	-76	E	8	7	360531.520	100	70	E	8	7	360531.520	100	70	E	8	7	360531.520	100	70	E	8	7	360531.520	100	70	E	8	7	360531.520	100	70	E
8	7	361644.170	100	-80	E	11	10	495773.436	100	-48	O	11	10	495773.436	100	-48	O	11	10	495773.436	100	-48	O	11	10	495773.436	100	-48	O	11	10	495773.436	100	-48	O
11	10	496863.268	100	-17	O	11	10	495773.436	100	-48	O	11	10	495773.436	100	-48	O	11	10	495773.436	100	-48	O	11	10	495773.436	100	-48	O	11	10	495773.436	100	-48	O

observed, possibly reflecting the influence of higher order Hamiltonian terms or interaction with the $K = -3$ levels which would act to push the $K = -1$ levels further down.

The strong coupling and mixing among the substates indicated by Fig. 1 also created difficulties within the fitting program in assigning consistent K labels to the Hamiltonian eigenvalues and correctly keeping track of each particular series of substate levels with increasing J value. Originally, a number of FTFIR lines involving the levels with $J > 16$ labeled as $K = 0$ or $K = -1$ E had conspicuously large residuals so were removed from the fit. However, the magnitudes of the residuals were quite consistent at 0.172 and 0.165 cm^{-1} for $J = 17$ and 18, respectively, and on inspection turned out to be precisely the separations between $K = 0$ and -1 term values for those J states. A plot of the computer-generated energies was virtually identical to Fig. 1a but had a “level crossing” between $J = 16$ and $J = 17$ due to interchange by the program of the $K = 0$ and -1 labeling for $J \geq 17$. Thus, simply switching the $K = 0$ and -1 assignments for $J \geq 17$ sufficed to solve the problem and bring the residuals back down to experimental accuracy. (Note that both the original and the reversed assignments are shown in the archived FTFIR data set, in order to highlight the K -labeling problem and to emphasize the successful modeling of these lines with the K -ordering reversed.)

The only other major discrepancies between observed and calculated wavenumbers in the fit occurred for the $(v_i, K, J) = (1, 0, 18) \leftarrow (0, 1, 17)$ E transition, with a residual of -0.14249 cm^{-1} , and the $(1, -1, 13) \leftarrow (0, -2, 14)$ and $(1, -1, 14) \leftarrow (0, -2, 14)$ E transitions with residuals of

0.07329 and 0.07297 cm^{-1} , respectively, as seen in the archived data. Each of these lines was the last identified member of its particular series in the spectrum, suggesting that the literature assignments had gone off track at those points. We realized that we could explicitly check for this by using published IR wavenumbers for the CO-stretching band (20) to determine $K = 1$ and -2 E $v_i = 0$ ground state combination differences. These were then matched against the corresponding combination differences calculated with ground state term values obtained from analysis of the assigned FIR lines using the Ritz fitting program (27). We found that to reproduce the CO-stretching IR combination differences, the $(0, 1, 17)$ and $(0, -2, 14)$ E energies indeed needed to be adjusted by -0.1418 and $+0.0732 \text{ cm}^{-1}$, as implied from the residuals in the fit, showing that the global analysis is correctly modeling these levels.

As implied above, the large asymmetry shifts and mixing of the five strongly coupled $K = 0$ to ± 2 $v_i = 0$ E substates make detailed calculation of transitions involving their sublevels a rigorous test for the global fitting program. However, our current corrected $(\nu_{\text{obs}} - \nu_{\text{calc}})$ residuals for these transitions show no features unaccounted for, and the perturbed subbands are well reproduced. With respect to the question of whether the $K = 0$ and -1 $v_i = 0$ E levels start to slowly diverge again above $J = 18$ as our analysis predicts, an extrapolation of the $K = 0$ and -1 E series using the IR ground state combination differences indicates that this is in fact the case, and that the energies are well modeled by the calculations based on the parameters of Table 1.

TABLE 4
CH₃OD MW and MMW $\nu_t = 2 \leftarrow 2$ *a*-Type Transitions of *A* and *E* Torsional Symmetry for $J \leq 20$ with Observed Minus Calculated Residuals Obtained Using the Global Fit Parameters of Table 1

J'	P'	J''	P''	Freq (MHz)	O-C (MHz)	Ref	J'	J''	Freq (MHz)	O-C (MHz)	Ref	J'	J''	Freq (MHz)	O-C (MHz)	Ref		
K = 0 ← 0							K = -7 ← -7					K = 1 ← 1						
1	+	0	+	45193.740	0.5	A	11	10	496706.629	6.5	O	2	1	90368.920	1.7	A,E		
2	+	1	+	90386.350	1.0	A,E	K = -6 ← -6					3	2	135551.990	2.7	A,E,O		
3	+	2	+	135576.810	1.4	A,E,O	11	10	498153.565	-1.8	O	4	3	180733.150	3.5	A,E		
4	+	3	+	180764.110	1.9	A,E	K = -4 ← -4					5	4	225912.050	4.4	E		
5	+	4	+	225947.170	2.4	E	5	4	225832.190	-133.2	E	6	5	271087.990	5.3	E		
6	+	5	+	271124.910	2.9	E	6	5	270991.360	-166.7	E	7	6	316260.190	6.1	E		
7	+	6	+	316296.320	3.4	E	7	6	316146.500	-203.9	E	8	7	361428.290	6.9	E		
8	+	7	+	361460.210	3.8	E	8	7	361297.070	-245.4	E	11	10	496901.442	8.9	O		
11	+	10	+	496896.727	5.0	O	K = -3 ← -3					K = 2 ← 2						
K = 1 ← 1							4	3	180712.500	2.4	A,E	3	2	135628.150	1.8	E,O		
2	+	1	+	89707.610	0.7	A,E	5	4	225885.420	3.0	E	4	3	180831.790	2.3	E		
3	+	2	+	134559.300	0.9	E,O	6	5	271054.920	3.6	E	5	4	226030.500	2.8	E		
4	+	3	+	179408.810	1.3	E	7	6	316220.250	4.3	E	6	5	271223.090	3.3	E		
5	+	4	+	224255.060	1.6	E	8	7	361380.730	5.0	E	7	6	316408.500	3.9	E		
6	+	5	+	269097.340	2.0	E	K = -2 ← -2					8	7	361585.250	4.3	E		
7	+	6	+	313934.890	2.4	E	3	2	135586.910	1.2	A,E,O	11	10	497052.373	5.5	O		
8	+	7	+	358766.870	2.7	E	4	3	180776.260	1.6	A,E	K = 3 ← 3						
11	+	10	+	493221.915	4.0	O	5	4	225960.290	2.2	E	4	3	180674.120	2.3	E		
2	-	1	-	91064.220	1.5	A	6	5	271137.400	2.6	E	5	4	225834.640	2.8	E		
3	-	2	-	136593.950	2.1	E,O	7	6	316306.440	3.0	E	6	5	270989.880	3.5	E		
4	-	3	-	182120.910	2.8	E	8	7	361466.020	3.5	E	7	6	316138.630	4.0	E		
5	-	4	-	227644.200	3.5	E	11	10	496878.940	9.1	O	8	7	361279.990	4.6	E		
6	-	5	-	273162.830	4.2	E	K = -2 ← -1					11	10	496647.032	4.6	O		
7	-	6	-	318675.900	5.0	E	3	2	607125.533	-12.0	O	K = 4 ← 4						
8	-	7	-	364182.640	5.8	E	K = -1 ← -1					5	4	225911.360	2.5	E		
K = 2 ← 2							2	1	90381.110	1.0	A,E	7	6	316262.170	3.4	E		
3	+	2	+	135528.060	2.3	A,E,O	3	2	135568.641	1.1	O	8	7	361432.780	4.0	E		
4	+	3	+	180701.680	3.1	A,E	4	3	180754.100	2.1	E	11	10	496919.320	6.0	O		
5	+	4	+	225873.050	3.8	E	5	4	225935.080	2.7	E	K = 5 ← 5						
6	+	5	+	271041.880	4.6	E	6	5	271110.940	3.2	E	11	10	496832.855	8.9	O		
7	+	6	+	316207.570	5.5	E	7	6	316280.680	3.8	E	K = 7 ← 7						
8	+	7	+	361369.620	6.3	E	8	7	361443.330	4.3	E	11	10	495490.452	14.1	O		
11	+	10	+	496832.855	13.7	O	11	10	496874.621	1.6	O							
3	-	2	-	135526.270	2.3	A,E,O	K = 0 ← 0											
4	-	3	-	180697.270	3.1	A,E	1	0	45190.130	0.7	A							
5	-	4	-	225864.350	3.8	E	2	1	90379.720	1.3	A							
6	-	5	-	271026.680	4.6	E	3	2	135568.970	2.4	A,O							
7	-	6	-	316183.260	5.4	E	4	3	180756.340	2.7	A							
8	-	7	-	361333.100	6.1	E	5	4	225942.390	3.3	E							
11	-	10	-	496732.626	8.4	O	6	5	271126.540	4.0	E							
K = 3 ← 3							7	6	316308.360	4.8	E							
11	+	10	+	494939.701	2.6	O	8	7	361487.180	5.4	E							
11	-	10	-	494939.701	2.7	O	11	10	497002.975	7.2	O							
K = 6 ← 6																		
11	+	10	+	496647.032	14.6	O												
11	-	10	-	496647.032	14.6	O												
K = 9 ← 9																		
11	+	10	+	498232.131	2.7	O												
11	-	10	-	498232.131	2.7	O												

Note: Refs.: A, (9); E, (13); O, new Ohio State FASSST measurements.

IV. DISCUSSION AND CONCLUSIONS

In this work on the $\nu_t = 0$ and 1 ground state spectrum of the CH₃OD isotopic species of methanol, new measurements and line assignments have been obtained in the MMW and

MW spectral regions and have been incorporated into a large data set of 564 MW and MMW lines and 4664 FTFIR lines. Global analysis of this data set has been accomplished with an overall weighted standard deviation of 1.060, i.e., essentially to

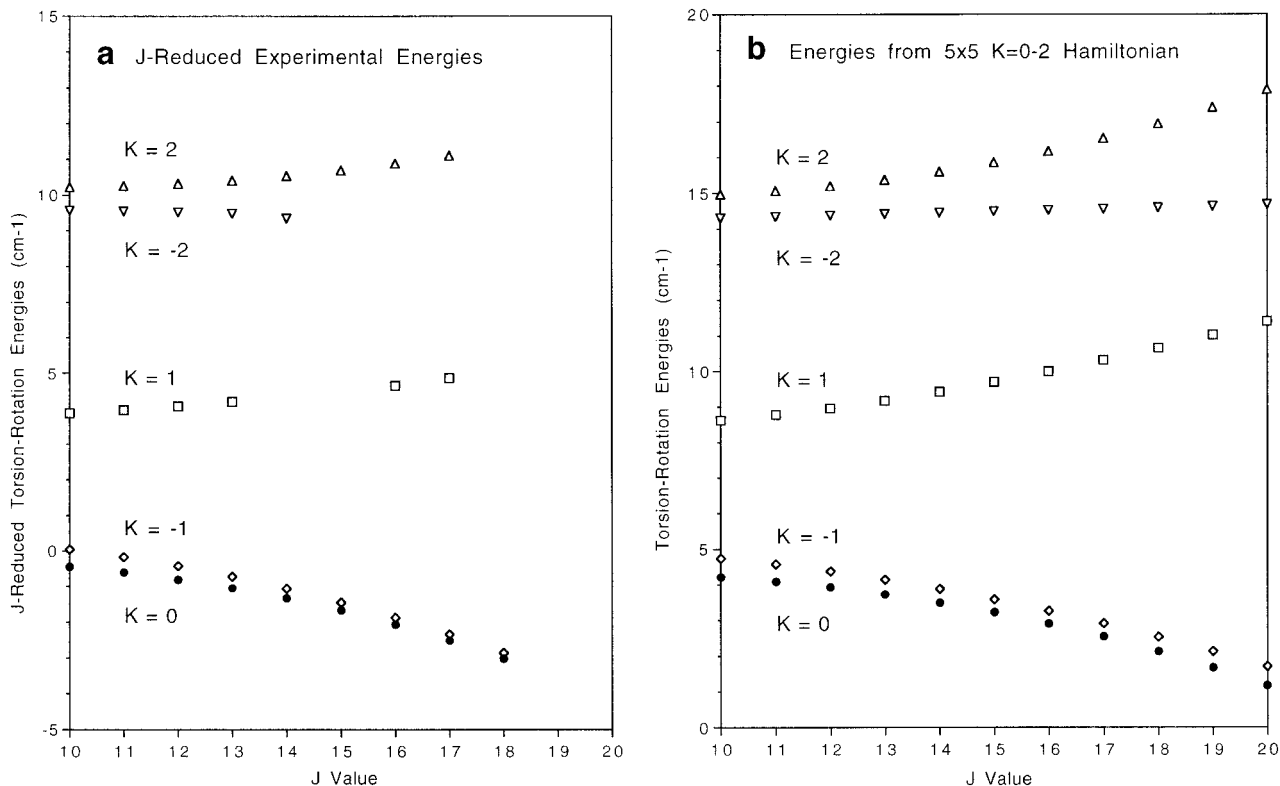


FIG. 1. (a) Plot of J -reduced experimental torsion-rotation energies for the $K = 0 - \pm 2 E v_t = 0$ substates of CH_3OD , obtained by subtracting $BJ(J + 1)$ from the term values using a mean B value of 0.7576 cm^{-1} . (b) Torsion-rotation energies for the $K = 0 - \pm 2 E v_t = 0$ substates of CH_3OD calculated from a simple 5×5 Hamiltonian taking the $J = 2$ term values as the unperturbed energies and introducing $\Delta K = \pm 1$ and $\Delta K = \pm 2$ asymmetry matrix elements evaluated with $D_{ab} = 840.8 \text{ MHz}$ and $(B - C) = 1483.2 \text{ MHz}$, respectively.

within mean experimental uncertainty, using a torsion-rotation model with 53 adjustable parameters and including terms of up to sixth order in the torsion-rotation operators. The new MMW measurements, plus the results of the fit in the form of the full dataset together with the least-squares ($\nu_{\text{obs}} - \nu_{\text{calc}}$) residuals, have been deposited as supplementary information in the JMS archive, accessible from the JMS home page at www.idealibrary.com.

There is good internal consistency among the parameter sets obtained here for CH_3OD and previously for $^{12}\text{CH}_3\text{OH}$ (2), $^{13}\text{CH}_3\text{OH}$ (3), and CD_3OH (4). This reinforces confidence in the fitting procedure, suggesting that the right minima are being found in the least-squares process and that the parameter reliability will permit meaningful intercomparison. Furthermore, recent *ab initio* calculations using the Gaussian program to explore structural relaxation when going from the bottom to the top of the torsional barrier (30) have shown promising agreement with the global fitting results for $^{12}\text{CH}_3\text{OH}$ for those distortional terms having a $(1 - \cos 3\gamma)$ functional dependence.

Altogether, we have now achieved global fits for the $v_t = 0$ and 1 torsional states of CH_3OH , $^{13}\text{CH}_3\text{OH}$, CD_3OH , and CH_3OD for $J \leq 20$ over the full available K value ranges. The parameter sets have been used to calculate reliable ground state energies which have proven to be extremely valuable for the

assignment of IR vibrational bands through the use of ground state combination differences.

Planned extensions to the program of global fitting include a move upward in energy to torsional states with $v_t \geq 2$ in order to test the one-dimensional Hamiltonian model in the near free-rotor regime above the barrier. Once the lower levels of the ground state are firmly under control, we will be in a position to explore coupled-state analysis of the vibrational perturbations that enter the problem when high v_t ground state levels interact with $v_t = 0$ and 1 states of the small-amplitude vibrations. We will also extend our global fitting to additional methanol isotopomers for which large spectroscopic data sets exist, in order to probe further the isotopic dependence of the parameters. At present, the encouraging convergence of experimental spectroscopy and theoretical *ab initio* techniques (30–32) holds promise for detailed understanding of the isotopic results and quantitative interpretation of many of the Hamiltonian parameters.

ACKNOWLEDGMENTS

The authors thank Drs. I. Kleiner and M. Godefroid for making their acetaldehyde (CH_3CHO) internal-rotation global-fitting program available for this work, and Dr. Jon T. Hougen for his continuing interest in the project. We

are grateful for financial support from the Natural Sciences and Engineering Research Council of Canada and the University of New Brunswick Research Fund (L.H.X. and R.M.L.), from MURST, Rome (G.M.), and from NASA (S.A., R.A.H.B., and F.C.D.).

REFERENCES

1. Li-Hong Xu and J. T. Hougen, *J. Mol. Spectrosc.* **169**, 396–409 (1995).
2. Li-Hong Xu and J. T. Hougen, *J. Mol. Spectrosc.* **173**, 540–551 (1995).
3. Li-Hong Xu, M. S. Walsh, and R. M. Lees, *J. Mol. Spectrosc.* **179**, 269–281 (1996).
4. M. S. Walsh, Li-Hong Xu, and R. M. Lees, *J. Mol. Spectrosc.* **188**, 85–93 (1998).
5. I. Kleiner and M. Godefroid, private communication.
6. E. Herbst, J. K. Messer, F. C. DeLucia, and P. Helminger, *J. Mol. Spectrosc.* **108**, 42–57 (1984).
7. I. Kleiner, J. T. Hougen, J.-U. Grabow, S. P. Belov, M. Yu. Tretyakov, and J. Cosleou, *J. Mol. Spectrosc.* **179**, 41–60 (1996). [See references therein.]
8. P. Venkateswarlu, H. D. Edwards, and W. Gordy, *J. Chem. Phys.* **23**, 1195–1199 (1955).
9. R. M. Lees and J. G. Baker, *J. Chem. Phys.* **48**, 5299–5318 (1968).
10. V. K. Kaushik, K. Takagi, and C. Matsumura, *J. Mol. Spectrosc.* **82**, 418–426 (1980).
11. K. Takagi and V. K. Kaushik, *J. Mol. Spectrosc.* **93**, 438–440 (1982).
12. T. Anderson, R. L. Crownover, E. Herbst, and F. C. DeLucia, *Astrophys. J. Suppl.* **67**, 135–148 (1988).
13. T. Anderson, E. Herbst, and F. C. DeLucia, *J. Mol. Spectrosc.* **159**, 410–421 (1993).
14. D. R. Woods, Ph.D. thesis, University of Michigan, Ann Arbor, MI, 1970.
15. Y. Y. Kwan and D. M. Dennison, *J. Mol. Spectrosc.* **43**, 291–319 (1972).
16. I. Mukhopadhyay, P. K. Gupta, G. Moruzzi, B. P. Winnewisser, and M. Winnewisser, *J. Mol. Spectrosc.* **186**, 15–21 (1997).
17. I. Mukhopadhyay, Y. B. Duan, and K. Takagi, *Spectrochim. Acta, Part A* **54**, 1325–1335 (1998).
18. I. Mukhopadhyay, *Spectrochim. Acta, Part A* **55**, 1767–1791 (1999).
19. Y. B. Duan and A. B. McCoy, *J. Mol. Spectrosc.* **199**, 302–306 (2000).
20. A. Lundsgaard, J. C. Petersen, and J. Henningsen, *J. Mol. Spectrosc.* **167**, 131–155 (1994).
21. M. Jackson, G. R. Sudhakaran, A. Silveira, Jr., I. Mukhopadhyay, and R. M. Lees, *Int. J. Infrared Millimeter Waves* **20**, 583–594 (1999).
22. D. T. Petkie, T. M. Goyette, R. P. A. Bettens, S. P. Belov, S. Albert, P. Helminger, and F. C. DeLucia, *Rev. Sci. Instrum.* **68**, 1675–1683 (1997).
23. Li-Hong Xu and F. J. Lovas, *J. Phys. Chem. Ref. Data* **26**, 17–156 (1997).
24. M. S. Walsh, M.Sc. thesis, University of New Brunswick, 1999.
25. F. J. Lovas, private communication.
26. R. M. Lees, unpublished data.
27. G. Moruzzi, Li-Hong Xu, R. M. Lees, B. P. Winnewisser, and M. Winnewisser, *J. Mol. Spectrosc.* **167**, 156–175 (1994).
28. G. Moruzzi and Li-Hong Xu, *J. Mol. Spectrosc.* **165**, 233–248 (1994).
29. I. Mukhopadhyay, Y. B. Duan, X. T. Wu, and K. Takagi, *Spectrochim. Acta, Part A* **56**, 19–28 (1999).
30. Li-Hong Xu, R. M. Lees, and J. T. Hougen, *J. Chem. Phys.* **110**, 3835–3841 (1999).
31. A. Chung-Phillips and K. A. Jebber, *J. Chem. Phys.* **102**, 7080–7087 (1995).
32. J. Florian, J. Leszczynski, B. G. Johnson, and L. Goodman, *Mol. Phys.* **91**, 439–447 (1997).